A New Impedance Control Method Using Backstepping Approach for Flexible Joint Robot Manipulators

Zhao-Hui Jiang
Hiroshima Institute of Technology, Hiroshima, Japan
Email: jiang@cc.it-hiroshima.ac.jp

Tetsuya Irie
THK Corporation, Tokyo, Japan

Abstract— **In this paper, we propose a new impedance control method for flexible joint robot manipulators. An ideal nonlinear impedance dynamic model is formulated in the workspace. Three control strategies that meet the requirement of desired impedance dynamics and stability of the whole system are derived by using backstepping control approach. The control system has a cascade structure with the designed three control strategies serially connecting to each other. Stability of the closed-loop system is analyzed using Lyapunov stability theory. Impedance control experiments are carried out on a 2-link flexible joint robot manipulator with a force sensor equipped at the end-effector. The results demonstrate the effectiveness of the proposed impedance control method.**

Index Terms— **impedance control, workspace, flexible joint robot, backstepping approach, stability analysis**

I. Introduction

Impedance control of robot systems has a significant advantage: it can change dynamic behavior of the robot just like a mass-spring-dashpot system when the robot responses to the interactive force acting at its end-effector. The impedance control concept was introduced by N. Hogan [1]. Since then, this issue has attracted many attentions.

Recently, impedance control has been adopted for the development of rehabilitation robotic systems, since it can improve safety of the system, and furthermore regulate the interaction force between the robot and human body. Implementation of an impedance controller in a robotic platform for ankle rehabilitation based on a Markovian approach was presented [2]. An asymptotically stable stiffness and impedance controller was designed based on the Lyapunov approach for robot-aided rehabilitation [3]. A variable impedance control method for a lower-limb rehabilitation robotic system using fuzzy logic and voltage control strategy was presented [4]. On impedance control of robots with structural flexibility, however, only a few research results have been reported. An adaptive impedance control method for multi-joint flexible link robot manipulator was proposed. This method is based on the tracking of a targeted trajectory generated by designed impedance dynamics in the presence of contact force [5]. An impedance controller for flexible joint robots was proposed with inner loop torque feedback and outer loop impedance control. The target impedance was designed with desired stiffness and damping [6].

On control design techniques for the flexible joint robot, recent years, backstepping control method interests many researchers. A backstepping method for tracking control of multi-joint variable stiffness robots was presented [7]. An output feedback control based on the backstepping approach was proposed. The control method guarantees asymptotic stability of the flexible joint robot system [8]. A workspace trajectory control method using an ideal manifold for multi-link flexible joint robots was proposed based on backstepping approach [9].

In this paper, a new impedance control method based on backstepping approach is proposed for multi-link flexible joint robots. Based on this method, the control design can be broken down into two stages stated as follows. First, a target nonlinear impedance model is designed in the workspace to prescribe ideal impedance performance of the robot. Second, three control schemes are designed using the backstepping control approach for impedance control in the workspace and vibration suppressing in the joint space. Stability of the system is analyzed based on Lyapunov stability theory. Impedance control experiments with external force acting at the end-effector are carried on a two-link flexible robot made by Quanser Corporation with a six axes force sensor made by Nitta Corporation equipped at the distal end of the robot. The results demonstrate the effectiveness of the proposed impedance control method.

This paper is organized as follows. Dynamic models of the robot in joint space and workspace are given in Section 2. Section 3 describes the design of the ideal nonlinear impedance model in the workspace. Section 4 presents the details of control system design. Stability analysis is given in Section 5. Section 6 demonstrates the

Manuscript received July 3, 2019; revised May 14, 2020

doi: 10.18178/ijmerr.9.6.865-869

impedance control experimental results. Finally, conclusions are stated in Section 7.

II. Dynamics Modeling

Consider an n-link flexible joint robot manipulator, each joint being modeled as a liner rotation spring between the actuator and the link driven by the joint. The mass and moment of inertia of the transmission are equivalently added to both sides of the actuator and link. In this section, dynamics of n-link flexible joint robot manipulators is presented in the joint space. In order for us to design the control system in the workspace easier the dynamics is then transformed to the workspace.

A. Joint Space Dynamics

Dynamics of the robot system is derived based on Lagrange's formulation. When an external force acts at the end-effector, motion equations of the robot can be given as follow.

$$M_L(\theta)\ddot{\theta} + D_L(\theta,\dot{\theta})\dot{\theta} - K(\theta_M - \theta) + g_L(\theta) = J^T(\theta)F \tag{1}$$

$$I_M\ddot{\theta}_M + K(\theta_M - \theta) = u\ . \tag{2}$$

(1) and (2) are joint motion equations on the link side and the motor side, respectively. $\theta_M \in R^n$ is the motor side joint variable, and $\theta \in R^n$ is its link side counterpart. $M_L(\theta) \in R^{n\times n}$ and $D_L(\theta,\dot{\theta})\dot{\theta} \in R^n$ denote the inertia matrix, and Coriolis and centrifugal forces; $K\in R^{n\times n}$ and $g_L(\theta) \in R^n$ are the matrix of stiffness and gravity. $I_M \in R^{n\times n}$ is moment of inertia of the joint shaft, $u \in R^n$ is the joint control torque. $J^T(\theta) \in R^{n\times N}$ and $F \in R^N$ denote the transpose of Jacobian and external force acting at the end-effector, respectively.

Remarks:

It should be noticed that the flexible joint robot has following important properties.

(i) $M_L(\theta)$ is a positive definite symmetric matrix;

(ii) $\frac{1}{2}\dot{M}_L(\theta) - D_L(\theta,\dot{\theta})$ is a skew symmetric matrix.

B. Dynamics Described in the Workspace

Since we are dealing with workspace impedance control, first of all we need to transform the dynamic model given in section 2.1 into the workspace. To do so, we analyze kinematics of the robot. As end-effector motion of the robot is only determined by link side joint variableθ, kinematic relations can be given as follows.

$$P = f(\theta) \tag{3}$$

$$\dot{P} = J(\theta)\dot{\theta} \tag{4}$$

$$\ddot{P} = J(\theta)\ddot{\theta} + \dot{J}(\theta)\dot{\theta} \tag{5}$$

where $P \in R^N$ is the end-effector position vector, $\dot{P}$ and $\ddot{P}$ are the velocity and acceleration, respectively. $f(\theta)$ is a nonlinear function vctor.

We transform motion equation (1) to the workspace while leaving motion equation (2) unchanged in the joints pace. As the result, equation (1) becomes.

$$M_p(\theta)\ddot{P} + D_p(\theta,\dot{\theta})\dot{P} + h_p(\theta,\dot{\theta}) = J^{-T}(\theta)K(\theta_M - \theta) + F\ . \tag{6}$$

Here

$$M_P(\theta) \equiv J^{-T}(\theta)M_L(\theta)J^{-1}(\theta) \tag{6a}$$

is the generalized matrix of inertia.

$$D_P(\theta,\dot{\theta})\dot{\theta} \equiv J^{-T}(\theta)D_L(\theta,\dot{\theta})J^{-1}(\theta)\dot{\theta} \tag{6b}$$

and

$$h_p(\theta,\dot{\theta}) \equiv J^{-T}(\theta)\{g_L(\theta) - M_L(\theta)J^{-1}(\theta)\dot{J}(\theta)\dot{\theta}\} \tag{6c}$$

are Coriolis and centrifugal forces in the workspace, and gravity together with the nonlinear forces cause by the coordinate transformation.

Remarks:

(iii) Since $M_L(\theta)$ is positive-definite symmetric, $M_P(\theta)$ is also positive-definite symmetric.

(iv) Since $\frac{1}{2}\dot{M}_L(\theta) - D_L(\theta,\dot{\theta})$ is skew symmetric, it is easy to prove that $\frac{1}{2}\dot{M}_P(\theta) - D_P(\theta,\dot{\theta})$ is also skew symmetric.

Property (iv) is especially important for the control design and stability analysis.

C. The Ideal Impedance Dynamics

The impedance control issue addressed in this paper is formulated as an end-effector trajectory tracking problem with reaction force from the environment acting at the end-effector. The ideal impedance model is designed as an N dimensional nonlinear impedance dynamic equation described as follows.

$$M_P(\theta)\Delta\ddot{P} + (D_P(\theta) + D_d)\Delta\dot{P} + K_d\Delta P = F \tag{7}$$

where $\Delta P \in R^N$ is end-effector trajectory tracking error defined as $\Delta P = P - P_d$. P and P_d are end-effector position vector and planned end-effector trajectory; $\Delta\dot{P}$ and $\Delta\ddot{P}$ are velocity and acceleration errors accordingly. D_d , and K_d are damping, stiffness matrices, they are designed as positive-definite constant diagonal matrices. Each diagonal element of the matrices relates to the direction of a specific axis of the workspace coordinate system. Therefore, the elements of D_d, and K_d can be designed separately and independently in each direction of the workspace. Here, we adopt the generalized matrix of inertia $M_p(\theta)$ as the ideal mass matrix, and $D_P(\theta) + D_d$ as the total damping matrix.

III. Design of Control Schemes

The main difference between the flexible joint robot and its ordinary counterpart is that links of the former is not directly driven by the actuators but through the joint flexible behavior. Hence, the control design should focus on two issues: one is how to cause such the joint flexible behavior that it meets the requirements of desired impedance dynamics, another one is how to dampen vibration of the flexible link to ensure stability of the system.

In this section, we derive the control strategy based on backstepping control approach.

A. The First Control Scheme

In (6), we define the elastic torque as a nominal control input of the subsystem and rewritten (6) as follows.

$$M_p(\theta)\ddot{P} + D_p(\theta,\dot{\theta})\dot{P} + h_p(\theta,\dot{\theta}) = J^{-T}(\theta)\tau + F \quad (8)$$

where

$$\tau = K(\theta_M - \theta) \quad (9)$$

is the nominal control input.

The design of the first control scheme is concentrated on changing dynamics of subsystem (8) such that it meets impedance dynamics (7). In detail, the control scheme is given as below.

$$\tau_d = J^T(\theta)\{v + D_P(\theta,\dot{\theta})\dot{P} + h_p(\theta,\dot{\theta})\} \quad (10)$$

where

$$v = M_P(\theta)\ddot{P}_d - D_d\,\Delta\dot{P} - K_d\Delta P \quad . \quad (11)$$

Under this control scheme, subsystem (6) becomes

$$M_P(\theta)\Delta\ddot{P} + (D_P(\theta) + D_d)\Delta\dot{P} + K_d\Delta P = F + J^{-T}(\theta)e_\tau \quad (12)$$

where $e_\tau \equiv \tau - \tau_d$ denotes the error between the real elastic torque and the designed nominal control input given by (10).

B. The Second Control Scheme

The objective of the second control scheme design is to ensure that the error of the first control input e_τ converges to zero. To do so, we take time derivative of (9) to have

$$\dot{\theta}_M = K^{-1}\dot{\tau} + \dot{\theta} \quad (13)$$

The second control scheme is designed to prescribe the desired joint motion on the motor side so that the abovementioned objective can be realized. The details are given as follows.

$$\dot{\theta}_{Md} = K^{-1}\left(\dot{\tau}_d - K_\tau(\tau - \tau_d) - J^{-1}(\theta)\Delta\dot{P}\right) + \dot{\theta} \quad (14)$$

where $K_\tau \in R^{n\times n}$ is a gain matrix that must be chosen as a positive-definite matrix.

Under control law (14) equation (13) becomes

$$\dot{e}_\tau + K_\tau e_\tau = Ke_\theta - J^{-1}(\theta)\Delta\dot{P}\,. \quad (15)$$

In (15), $e_\theta \equiv \dot{\theta}_M - \dot{\theta}_{Md}$ denotes the error between the real joint motion and desired joint motion.

C. The Third Control Scheme

The third control scheme is to guarantee that the real joint motion converges to the ideal joint motion. In detail, the control scheme is designed as

$$u = I_M\ddot{\theta}_{Md} - K_\theta\dot{e}_\theta + \tau_d \quad (16)$$

where $K_\tau \in R^{n\times n}$ is positive-definite feedback gain matrix. Under this control scheme, subsystem (2) becomes

$$I_M\dot{e}_\theta + K_\theta e_\theta + e_\tau = 0 \quad . \quad (17)$$

In above equation $K_\theta \in R^{n\times n}$ is a positive-definite gain matrix. It should be pointed out that the control input given by the third control law is the actual control input to the robot, and it combined the former two control schemes together.

In the control implementation, the first control scheme given by expressions (10) and (11) need to be firstly calculated based on the sensor signals and dynamic model described in (8). The second control law given by (14) is, then, calculated based on the first control scheme and its numerical differentiation. Finally the third control scheme, i.e., the actual control input given by (17) is computed using the first control scheme, and second control scheme together with its numerical differentiation. With these control schemes described above, it is seen that the impedance control system has a cascade structure.

IV. Stability Analysis

Stability analysis of the robot system takes place using Lyapunov stability theory. We consider Lyapunov function candidate without taking external forces into consideration as follows.

$$V = \tfrac{1}{2}\Delta\dot{P}^T M_p(\theta)\Delta\dot{P} + \tfrac{1}{2}\Delta P^T K_d\Delta P + \tfrac{1}{2}e_\tau^T e_\tau + \tfrac{1}{2}e_\theta^T K I_M e_\theta > 0 \quad (18)$$

Taking derivative with respect to time we obtain,

$$\dot{V} = \Delta\dot{P}^T M_p(\theta)\Delta\ddot{P} + \frac{1}{2}\Delta\dot{P}^T\dot{M}_p(\theta)\Delta\dot{P} + \Delta P^T K_d\Delta\dot{P} + e_\tau^T\dot{e}_\tau + e_\theta^T\dot{e}_\theta \quad (19)$$

Substituting solution trajectories of (12), (15) and (17) into (19) yields,

$$\begin{aligned}\dot{V} = {} & \Delta\dot{P}^T\left(J^{-T}(\theta)e_\tau - D_P(\theta)\Delta\dot{P} - D_d\Delta\dot{P} - K_d\Delta P\right) \\ & + \frac{1}{2}\Delta\dot{P}^T\dot{M}_p(\theta)\Delta\dot{P} + \Delta P^T K_d\Delta\dot{P} \\ & + e_\tau^T\left(Ke_\theta - J^{-1}(\theta)\Delta\dot{P} - K_\tau e_\tau\right) \\ & + e_\theta^T K(-K_\theta e_\theta - e_\tau)\end{aligned} \quad (20)$$

Since $\frac{1}{2}\dot{M}_P(\theta) - D_P(\theta,\dot{\theta})$ is a skew symmetric matrix, we obtain

$$\dot{V} = -\Delta\dot{P}^T D_d\Delta\dot{P} - e_\tau^T K_\tau e_\tau - e_\theta^T K K_\theta e_\theta < 0 \quad (21)$$

This completes the proof of stability of the impedance control system.

V. Impedance Control Experements

In order to demonstrate the effectiveness of the proposed control method, impedance control experiments are carried out on a 2-link flexible joint robot arm made by Quanser Corporation shown in Fig. 1. The main size and parameters of the robot are given in Table I. The rest parts of the dynamic parameters have been identified based on identification experiments. A six axes force sensor made by Nitta Corporation is set at the end of the robot arm to measure external forces acting at the end-effector. The force signals are transformed from the sensor coordinate system to the workspace using the homogenous transformation matrix.

Figure 1. 2-Link flexible joint robot with force sensor equipped at the end-effector

TABLE I. MAIN PARAMETERS OF THE ROBOT

Link length (m)	
Link1	0.343
Link2	0.267
Flexible joint rotational stiffness (N-m/rad)	
Joint1	9.0
Joint2	4.0

Three control schemes given in section 4 were used to establish the control system. In the design of impedance dynamics, we determined the damping and stiffness matrices as below

$$D_d = \mathrm{diag}[7.0, 7.0],$$

$$K_d = \mathrm{diag}[35.0, 35.0].$$

The feedback gain matrices were designed as follows.

$$K_\tau = \mathrm{diag}[3.8, 3.8],$$

$$K_\theta = \mathrm{diag}[4.5, 4.5].$$

The problem is prescribed as that contacting between the end-effector and environment takes place during end-effector trajectory tracking control. The end-effector trajectories are planned as a straight line in the workspace with trajectories on X and Y directions being planned as trigonometric functions as follows.

$$X_d = \frac{1}{2}(X_f - X_o) + X_o - \frac{1}{2}(X_f - X_o)\cos\left(\frac{\pi}{t_f}t\right),$$

$$Y_d = \frac{1}{2}(Y_f - Y_o) + Y_o - \frac{1}{2}(Y_f - Y_o)\cos\left(\frac{\pi}{t_f}t\right).$$

The velocity and acceleration trajectories are planned accordingly. Zero initial value and zero final value of velocities in both directions are preset. Experiments are carried out. The sampling time set as 1ms, and control time set as 5s.

Fig. 2 ~ Fig. 7 present the impedance control experimental result with external force acting at the end of the robot. The external force acts on the robot randomly by touching the sensor. Fig. 2 ~ Fig. 4 demonstrate that while tracking the planned end-effector trajectory the robot reacts to external force compliantly when the force appears. From Fig. 6 it is seen that vibration of the joints is damped effectively and stability of the system is ensured. The experimental result demonstrates that under the proposed control method, desired impedance performance of the robot control system can be guaranteed.

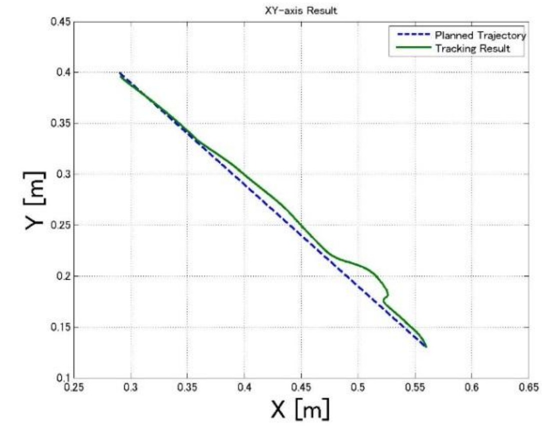

Figure 2. Planned trajectory and impedance control experimental result illustrated in the workspace with external force

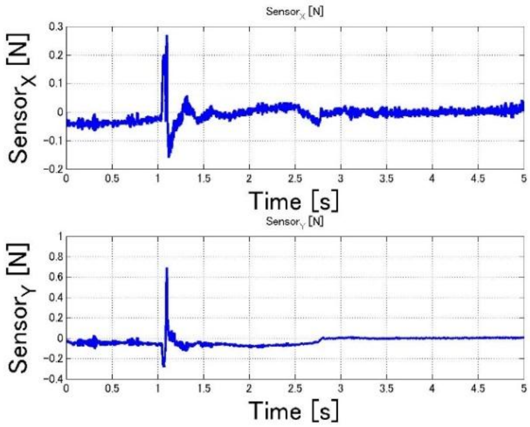

Figure 3. Workspace external force measured by the force sensor equipped at the end-effector.

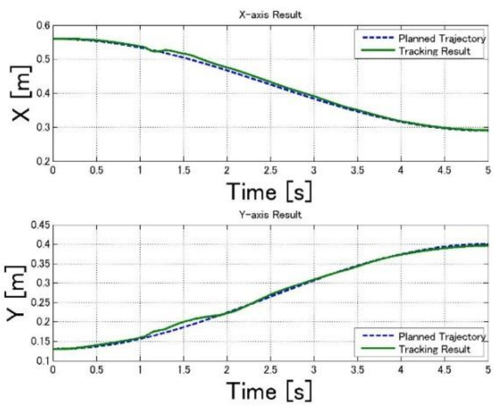

Figure 4. Time history of the planned end-effector trajectories and impedance control experimental results with external force

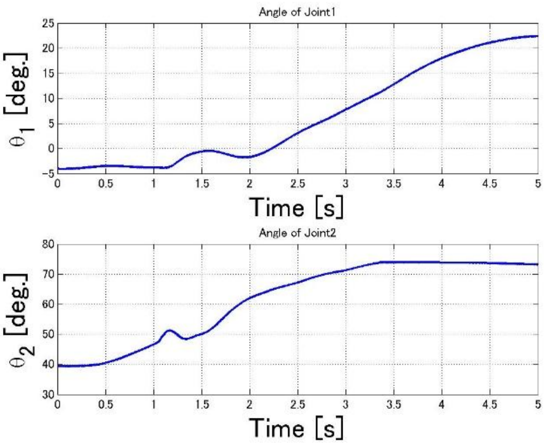

Figure 5. Time history of the joint responses during the impedance control process

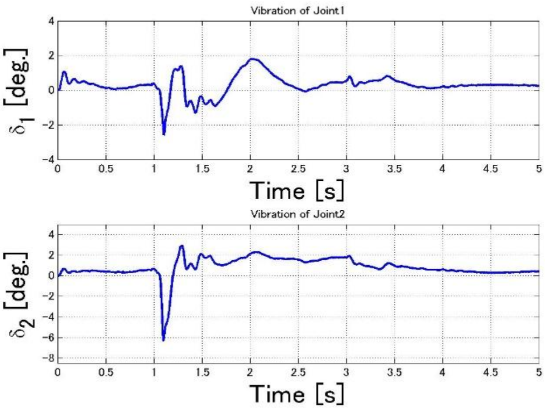

Figure 6. Time history of joint vibration

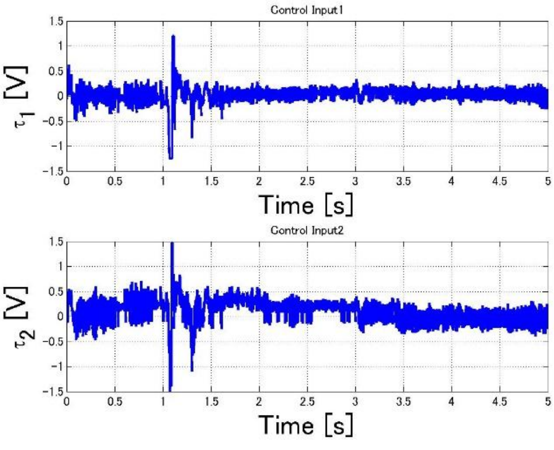

Figure 7. Time history of joint control inputs

Conflict of Interest

The authors declare no conflict of interest.

VI. Conclusions

This paper proposed a novel impedance control method for robot manipulators with joint flexibility. Three control schemes were designed based on the backstepping control approach to meet the requirement of desirable nonlinear impedance characteristics and stability of the system. Under the control schemes stability of the robot was analyzed using Lyapunov stability theory. A two-link flexible joint robot and a six axes force sensor equipped at the distal end of the robot arm were used as facility for experimental studies. Impedance control experiments were carried out. The results confirmed the fact that when external force does not exist the robot trucks preplanned end-effector trajectory and its joint vibration is damped effectively; when there appears an external force at the end-effector, the robot responses to the force compliantly. It demonstrates the effectiveness of the proposed impedance control method.

References

[1] N. Hogan, "Impedance control - An approach to manipulation. I - Theory," *Asme Transactions of Dynamic Systems & Measurement Control B* , vol. 107, pp. 304-313, 1984.

[2] A. L. Jutinico, J. C. Jaimes, F. M. Escalante, J. C. Perez-Ibarra, M. H. Terra, and A. G. Siqueira, "Impedance control for robotic rehabilitation: A robust Markovian approach," *Frontier in Neurorobotics*, vol. 11, Article43, pp. 1-16, 2017.

[3] H. Mehdi and O. Boubake, "Stiffness and impedance control using Lyapunov theory for robot-aided rehabilitation," *International Journal of Social Robotics*, vol. 4, Supplement 1, pp 107–119, 2012.

[4] V. Khoshdela, A. Akbarzadeh, and H. Moeenfard, "Variable impedance control for rehabilitation robot using interval type-2 fuzzy logic," *International Journal of Robotics*, vol. 4, no. 3, pp. 46-54, 2015.

[5] Z. H. Jiang, "Impedance control of flexible robot arms with parametric uncertainties," *Journal of Intelligent and Robotic Systems*, vol.42, no. 2, pp.113-133, 2005.

[6] C. Ott, A. Albu-Schaffer, and G. Hirzinger, "On the passivity-based impedance control of flexible joint robots," *IEEE Transactions on Robotics*, vol. 24, no. 2, pp. 416 – 429, 2008.

[7] F. Petit, A. Daasch, and A. Albu-Schäffer, "Backstepping control of variable stiffness robots," *IEEE Trans. on Control Systems Technology*, vol. 23, no. 6, pp. 2195-2202, 2015.

[8] A. Loria, S. Avila-Becerril, "Output-feedback global tracking control of robot manipulators with flexible joints," in *Proc. of American Control Conference*, pp. 4032-4037, 2014.

[9] Z. H. Jiang, and K. Shinohara, "Workspace trajectory tracking control of flexible joint robots based on backstepping method," in *Proc. IEEE TENCON*, pp. 3477-3480, 2016.

Zhao-Hui Jiang received his BS in mechanical engineering in 1982 from Harbin Institute of Technology, Harbin, China. He received his ME and Doctor degrees in mechanical engineering and precision engineering, in 1985 and 1988, from Chiba University, Chiba, Japan, and Tohoku University, Sendai, Japan, respectively.

He has been with Hiroshima Institute of Technology, Hiroshima, Japan since 1997, where he is currently professor in robotics and control engineering in the Department of Mechanical Systems Engineering.

Prof. Jiang is member of IEEE (AC, RA, and SMC), The Robotics Society of Japan, The Society of Instrument and Control Engineers, and The Japanese Society of Mechanical Engineers.

Tetsuya Irie received his BS and ME both from Hiroshima Institute of Technology, Hiroshima, Japan, in mechanical engineering, 2017 and 2019, respectively.

He joined THK Corporation, Tokyo, Japan, in April 2019, where he is now an engineer.